

QUALITATIVE AND QUANTITATIVE ANALYSIS OF SOILS USING LASER-INDUCED BREAKDOWN SPECTROSCOPY AND CHEMOMETRICS TOOLS **

V. C. Costa ^{1,2}, S. dos Santos Ferreira ³, L. N. Santos ³, M. A. Sperança ¹,
C. Santos da Silva ¹, G. A. Sodr e ³, E. R. Pereira-Filho ^{1*}

¹ Group of Applied Instrumental Analysis, Department of Chemistry, Federal University of S o Carlos, S o Carlos, S o Paulo State 13565-905, Brazil; e-mail: erpf@ufscar.br

² Laboratory of Toxicant and Drug Analyses (LATF), Federal University of Alfenas (Unifal), Alfenas, Minas Gerais State 37130-000 Brazil

³ State University of Santa Cruz, Ilh us, Bahia State 45662-900, Brazil

In the present work a method was proposed for the direct determination of Ca, Fe, K, and Mg and qualitative analysis of anthropized and cabruca soil samples from different depths (0–20 and 20–40 cm) by laser-induced breakdown spectroscopy (LIBS). The LIBS instrumental parameters were evaluated using a central composite design with a central point. The variables evaluated were as follows: delay time in five levels (0.5, 0.7, 1.2, 1.7, and 1.9 μs) and fluence at five levels (1448, 1811, 2659, 3514, and 3820 $\text{J}\cdot\text{cm}^{-2}$). The best results obtained were with a delay time of 1.2 μs and fluence of 2659 $\text{J}\cdot\text{cm}^{-2}$. The proposed calibration model for Ca, Fe, K, and Mg obtained using LIBS data presented a good correlation with the reference values obtained by inductively coupled plasma atomic emission spectrometry (ICP OES). In addition, multivariate data analysis from LIBS spectra in the region of 186–1042 nm was performed using principal component analysis (PCA). From the LIBS spectra it was possible to discriminate the different analyzed samples, showing that the combination of LIBS with PCA is an excellent option for the discrimination of soils.

Keywords: soil, LIBS, chemometric tools, qualitative analysis, quantitative analysis.

АНАЛИЗ ПОЧВ С ИСПОЛЬЗОВАНИЕМ ЛАЗЕРНО-ИНДУЦИРОВАННОЙ ИСКРОВОЙ СПЕКТРОСКОПИИ И ХЕМОМЕТРИКИ

V. C. Costa ^{1,2}, S. dos Santos Ferreira ³, L. N. Santos ³, M. A. Sperança ¹,
C. Santos da Silva ¹, G. A. Sodr e ³, E. R. Pereira-Filho ^{1*}

УДК 543.42:631.4

¹ Федеральный университет Сан-Карлос, Сан-Карлос, 13565-905, Бразилия; e-mail: erpf@ufscar.br

² Федеральный университет Альфенас, Альфенас, 37130-000, Бразилия

³ Государственный университет Санта-Крус, 45662-900, Ильеус, Бразилия

(Поступила 17 декабря 2018)

Предложен метод непосредственного определения Ca, Fe, K и Mg и качественного анализа образцов двух типов почв различной глубины (0–20 и 20–40 см) методом лазерно-индуцированной искровой спектроскопии (LIBS). Инструментальные параметры LIBS оценены с использованием центрально-композиционного плана с центральной точкой. Оценены следующие переменные: время задержки на пяти уровнях (0.5, 0.7, 1.2, 1.7 и 1.9 мкс) и флюенс на пяти уровнях (1448, 1811, 2659, 3514 и 3820 Дж/см²). Наилучшие результаты получены при времени задержки 1.2 мкс и плотности потока 2659 Дж/см². Предложенная калибровочная модель для Ca, Fe, K и Mg, полученная с использованием данных LIBS, дает хорошую корреляцию с эталонными значениями, полученными с помощью

** Full text is published in JAS V. 87, No. 2 (<http://springer.com/journal/10812>) and in electronic version of ZhPS V. 87, No. 2 (http://www.elibrary.ru/title_about.asp?id=7318; sales@elibrary.ru).

атомно-эмиссионной спектроскопии с индуктивно-связанной плазмой (ICP OES). Проведен многомерный анализ данных из спектров LIBS в области 186–1042 нм с использованием метода главных компонент (РСА). По спектрам LIBS можно выделить анализируемые образцы. Показано, что комбинация LIBS с РСА является отличным вариантом для различения почв.

Ключевые слова: почва, лазерно-индуцированная искровая спектроскопия, хемометрический инструмент, качественный анализ, количественный анализ.

Introduction. Soil quality and climate conditions are essential aspects for agriculture, defining characteristics of the crops and the generated products. Plants and soil maintain a relationship since plants absorb the nutrients for their development, and later, these nutrients return in the form of organic material to the soil. The nutritional composition of the soil affects the development of the plant [1]. In this scenario, the evaluation of nutrient concentration in soils is fundamental and can assist to ensure high productivity and the quality of crops.

In general, analytical techniques as atomic spectrometry are used for nutrient determination in soils [2]. However, these techniques require long sample preparation in order to convert the solid material to a homogeneous aqueous solution [3]. In contrast to the traditional sample preparation methods, direct analysis of the solid samples with minimal manipulation is an attractive alternative [4]. In this sense, laser-induced breakdown spectroscopy (LIBS) presents itself as an emerging analytical technique that shows great potential due to the possibility of analysis of the sample in its original form. In addition, it permits high analytical frequency and *in situ* analysis, which is interesting regarding soil analysis [5].

As far as soil analysis is concerned, LIBS has been used for different purposes [6, 7]. In the study proposed by Pontes et al. [8] LIBS was successfully used to classify different types of Brazilian soils (argisol, latosol, and nitosol). Ferreira et al. [9] determined Ba, Co, Cu, Mn, Ni, V, and Zn in two types of soils for studies related to sustainability, in which sewage sludge was applied as a fertilizer. In another study, Ferreira et al. [10] evaluated the humification degree of soil organic matter. Nicolodelli et al. [11] determined carbon content in soil samples from the Amazon region. On the other hand, Villas-Boas et al. [12] expanded the application of LIBS to soil texture analysis.

In a recent study, Zaytev et al. [13] determined Pb in soils using principal component regression (PCR) as a strategy for calibration. Ruhlmann et al. [14] quantified Ca in soils, comparing univariate and multivariate calibration strategies. The multivariate approach using partial least squares regression (PLSR) showed the best results.

Together with the LIBS applications, chemometric tools are used for the interpretation of its data [15]. Among the main chemometric tools used in LIBS, those related to multivariate optimization, as factorial design, Doehlert design, and central composite design, are the most used [16, 17]. These tools are employed to optimize the instrumental conditions of LIBS, such as delay time, spot size, and laser pulse fluence. Another chemometric tool widely used in LIBS is multivariate data analysis. This tool is increasingly applied to extract information from the vast amount of spectral data in LIBS. In particular, principal component analysis (PCA) is a multivariate exploratory data analysis most commonly employed in LIBS [15]. LIBS in combination with PCA has been applied for unsupervised classification of polymers [18], sediments [19], leather [20], and fertilizers [21]. The goal of this study is to develop a simple and fast method for the direct analysis of soil samples from different depths using LIBS for the determination of nutrients (Ca, Fe, K, and Mg), and qualitative analysis using PCA.

Experimental. Instrumentation. LIBS spectra were obtained using a J200 LIBS system (Applied Spectra, Fremont, CA, USA) controlled by Axiom 2.5 software (Applied Spectra). This instrument consists of a 1064 nm Nd:YAG laser and a 6-channel charge-coupled device (CCD) spectrometer recording spectral information from 186 to 1,042 nm. Channel 1 goes from 186 to 309 nm, channel 2 from 309 to 460 nm, channel 3 from 460 to 588 nm, channel 4 from 588 to 692 nm, channel 5 from 692 to 884 nm, and channel 6 from 884 to 1042 nm. The spectral resolution is <0.1 nm from UV to Vis and <0.12 nm from Vis to near infrared (NIR). Axiom 2.5 software from the same manufacturer controlled the operational parameters of the equipment. These parameters were the laser pulse energy, ranging from 0 to 100 mJ, the delay time, which is the time interval between the incidence of the laser pulse and the start of signal recording by the spectrometer, ranging from 0 to 2 μ s, and the spot size (diameter of the laser beam), ranging from 50 to 250 μ m. Axiom 2.5 software also manages the movement of the sample, assisted by an automated XYZ stage and a 1280 \times 1024 complementary metal-oxide semiconductor (CMOS) color camera imaging system. At 1.05 ms, the software establishes the gate width, which is the time the spectrometer registers the emission signals.

Inductively coupled plasma optical emission spectrometry (ICP OES) (iCAP 7000, Thermo Scientific, Waltham, MA, USA) was used as a comparative technique for the determination of Ca, Fe, K, and Mg. Argon gas (99.996%, White Martins-Praxair, Sertãozinho, SP, Brazil) was used to generate the plasma in all ICP OES measurements. The instrumental conditions were established as the manufacturer recommendations: power (1.2 kW), plasma gas flow (15.0 L/min), auxiliary gas flow (1.5 L/min), nebulizer gas flow (0.7 L/min), and sample introduction flow rate (2.1 ml/min). The elements and the emission lines monitored were Ca (317.933 nm), Fe (283.204 nm), K (766.465 nm), and Mg (280.270 nm).

Reagents and solutions. All solutions employed in the comparative ICP OES determinations were prepared using ultrapure water (18.2 M Ω cm resistivity) produced by a Milli-Q® Plus Total Water System (Millipore Corp., Bedford, MA, USA). Nitric acid (HNO₃), previously purified using a sub-boiling distillation system Distillacid™ BSB-939-IR (Berghof, Eningen, Germany), was used for the extractions of the analytes. All glassware and polypropylene flasks were washed with soap, soaked in 10% v/v HNO₃ for 24 h, and rinsed with deionized water prior to use. The multi-element standard solutions were prepared daily by appropriate dilution of 1000 mg/L Ca, Fe, K, and Mg stock solutions (Qhemis, Jundiaí, SP, Brazil) and used for construction of the calibration curves.

Sampling and samples. Soil samples were obtained in two distinct areas: (i) the soils from the first area are from the “cabruca” system, where cocoa is grown in consortium with the Atlantic Forest. (ii) the soils from the second area are derived from an “anthropized” system, where the soil is continuously removed by plowing. A total of sixteen samples was collected: 0–20 cm and 20–40 cm. For the soils of the “cabruca” system, four samples in depths of 0–20 cm (C1, C2, C3, and C4) and four samples in depths of 20–40 cm (C5, C6, C7, and C8) were collected. For the soils of the “anthropized system,” four samples in depths of 0–20 cm (A1, A2, A3, and A4) and four samples in depths of 20–40 cm (A5, A6, A7, and A8) were also collected.

Sample preparation for determination by ICP OES. ICP OES was used as a comparative technique to evaluate the accuracy of the LIBS proposed method. Calcium, Fe, K, and Mg were determined in soils after acid extraction of the samples. The analyte extractions were based on the method recommended by Brazilian legislation that follows the protocol established by the USA environmental agency, EPA 3051 [22, 23]. Approximately 200 mg of the sample was directly weighed in Teflon-PFA digestion vessels followed by the addition of 10 mL of 65% v/v HNO₃. The following microwave heating program was applied: (1) 5 min to reach 120°C; (2) 5 min hold at 120°C; (3) 5 min to reach 175°C, and (4) 10 min hold at 175 °C. The temperature was controlled by an infrared temperature sensor. After the extractions, the solutions were transferred to volumetric flasks, and high-purity water was added to achieve a total volume of 50 mL. In order to evaluate the accuracy of the extraction procedure, NIST CRM 2709 (San Joaquim soil) was submitted to the same procedure.

Multivariate optimization of LIBS parameters. Four soil samples (A1, A5, C1, and C5) were used to optimize the instrumental conditions used in the LIBS analysis. Approximately 250 mg of each sample was accurately weighed using an analytical balance (model AY 220, Shimadzu, Kyoto, Japan), and then pressed for 2 min under 80 kN to form pellets with a 12 mm diameter. The LIBS instrumental parameters were evaluated using a central composite design [24] with a central point. Four soils samples in pellets (A1, A5, C1, and C5) were used to optimize the instrumental conditions used in the LIBS analysis. The variables evaluated were as follows: laser pulse fluence (FL) at five levels (1448, 1811, 2659, 3514, and 3820 J/cm²) and delay time (DT) in five levels (0.5, 0.7, 1.2, 1.7, and 1.9 μ s). These values were selected taking into account the experimental range that can be modified in the LIBS instrument. For each pellet, three authentic replicates were prepared and approximately 400 spectra were obtained at different regions of the samples. These spectra were obtained in 10 lines, and in each one approximately 40 laser pulses were obtained. The following additional laser settings were used: a scan length of 8 mm, a laser repetition rate of 5.0 Hz, and a speed of 1.0 mm/s.

As a response to the central composite design, the area, height, and signal-to-background ratios (SBR) were evaluated using the most intense emission lines for Ca, Fe, K, and Mg. Each response was converted into values between 0 and 1 indicating an undesired and desired response, respectively. The individual desirability was combined into one single response (OD, overall desirability) [25]. Moreover, twelve signal normalization modes [20] were employed for data processing, and each mode was tested by an analysis of the pure error sum of squares (PESS). After the selection of the normalization mode, the best experimental condition was identified from high OD values.

Data collection and analytical parameters for the proposed method. Matlab software version 2018a (Mathworks, Natick, MA, USA) and two homemade routines were used for preliminary data inspection. The first routine, `libs_treat`, was applied to perform a visual data inspection and verify the presence of eventual outliers in the spectra. In this case, for each sample (rows in the data matrix), the standard deviation, area, maximum, and Euclidean norm were calculated. After this visual inspection we observed the individual spectrum to see what the problem was and after this confirmation, the spectrum was excluded from the original dataset. Afterwards, 12 normalization modes were calculated. This process was required because LIBS spectra were sensitive to several potential problems, including variations in the sample surface, the stability of the laser, and the interaction between the laser and the sample. The second routine, `libs_par`, was applied after normalization by `libs_treat`. LIBS_par enables the calculation of signal-to-background ratio (SBR) and both signal area and the height for a specified emission line. To use this routine, it is necessary to establish the emission line interval that contains the background and the signal [16, 26].

The efficiency of these normalizations was assessed during the optimization of the instrumental conditions of the LIBS system, observing the lowest PESS and for the proposition of calibration models using the lowest standard error of calibration (SEC). Additionally, the LIBS spectra were used for qualitative analysis of the soil samples. The multivariate data analysis was performed employing PCA to evaluate the relationship among emission lines and the samples. To achieve this, PCA was applied to the generated data matrix (16×12,288) with the samples organized in rows and emission lines (variables) in columns.

The limits of detection (LOD) and quantification (LOQ) were calculated according to three- and tenfold the standard deviation of the background noise, measured in the surroundings of the selected emission lines (Ca II 393.36, Fe II 259.94, K I 766.49, and Mg II 279.55), respectively, divided by the sensitivity of the calibration models proposed. In addition, the values of the standard of error validation (SEV) were also obtained.

Results and discussion. *Multivariate optimization of LIBS parameters.* Due to the interaction of electromagnetic radiation with matter, several phenomena occurred when the laser beam reached the sample surface. The laser sample interaction is extremely dependent on the sample matrix, surface, and analyte homogeneity. In addition, microplasma formation can be affected by the laser operating conditions (i.e., laser pulse energy, fluence, and duration), and the radiation emission characteristic of the species presented in this plasma (ions and molecules) can be influenced by instrumental parameters, such as delay time, gate width, amplification detector gain, and emission line selection. In this context, the instrumental parameters of the instrument must be optimized in order to minimize undesired effects during the analyzes [27].

In this sense, the instrumental conditions of the LIBS were studied in detail. Four soil samples (A1, A5, C1, and C5) and a central composite design were employed to evaluate the data. As a response to the central composite design, individual desirability values were obtained from the signal area, height, and SBR using the most intense emission line. In this case, each response was coded from 0 (undesired response; the lowest area, height, and SBR) to 1 (desired response; the highest area, height, and SBR). Therefore, the individual desirability values were combined into a single response using the geometric mean (OD, overall desirability). This process was repeated for each normalization, the regression models were calculated, and the first statistical parameter inspection was performed observing the PESS. The PESS reflects the aleatory error, and a suitable model should have a negligible error.

The normalizations evaluated were: (`norm_1`) the average of all the spectra; (`norm_2`) signal normalization by the norm, then, the average over all the spectra; (`norm_3`) signal normalization by the area, then, the average over all the spectra; (`norm_4`) signal normalization by the highest signal, then, the average over all the spectra; (`norm_5`) the sum of all spectra; (`norm_6`) signal normalization by the norm, then, the sum over all spectra; (`norm_7`) signal normalization by the area, then, the sum over all the spectra; (`norm_8`) signal normalization by the highest signal, then, the sum over all the spectra; (`norm_9`) signal normalization by the C I 193.09 nm emission line, then, the average over all the spectra; (`norm_10`) signal normalization by the C I 193.09 nm emission line, then, the sum over all the spectra; (`norm_11`) signal normalization by the C I 247.85 nm emission line, then, the average over all the spectra; (`norm_12`) signal normalization by the C I 247.85 nm emission line, then, the sum over all the spectra [16, 26].

Figure 1 shows the PESS values obtained after the application of the 12 normalization modes. It is possible to observe that normalization 9 (`norm_9`) presents the lowest PESS value, being selected to identify the best experimental conditions. When compared with normalization 1 (only average of the signals), normalization 9 provided a 5-fold reduction of the aleatory error. These normalizations were tested to compensate for signal variations (area or height) and the sample matrix differences during data acquisition.

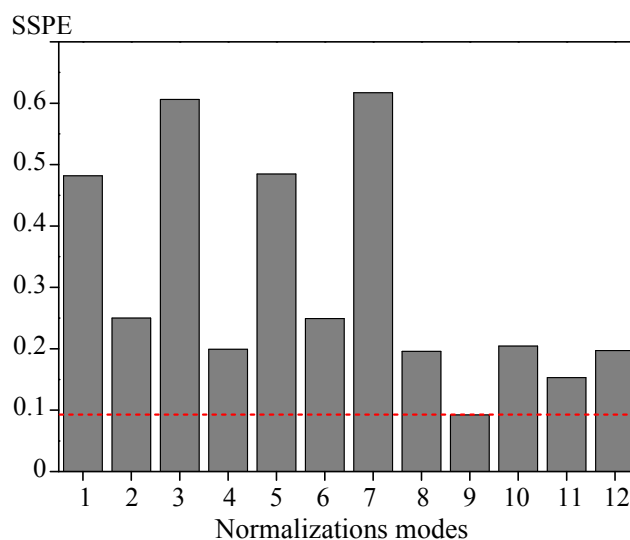


Fig. 1. Sum of Squares of pure error (SSPE) as a function of the 12 normalizations modes.

Table 1 presents the operating conditions for all the experiments performed, i.e., the eleven experiments that correspond to the selected experimental design, including triplicate at the central point. In addition, the responses in function of the OD using norm_9 are also shown. Subsequently a model was calculated, and analysis of variance (ANOVA) was applied to evaluate the lack of fit of the obtained models. After ANOVA table evaluation, six coefficients b_0 (constant), b_1 (FL), b_2 (DT), b_{11} (FL)², b_{22} (DT)², and b_{12} (DT×FL) were calculated; the coefficients b_1 , b_2 , b_{11} , and b_{12} were not significant at the 95% confidence level. Thus, the nonsignificant coefficients were removed, and the model was calculated again. The new model was statistically significant, by comparing the mean square of regression (MSR) and mean square of residue (MSr), the $F_{\text{calculated}}$ (30.65) being 6-fold higher than the $F_{\text{tabulated}}$ (5.12) at the 95% confidence level. On the other hand, the proposed model presented a lack of fit because the $F_{\text{calculated}}$ (35.95) for the ratio between the Mean square of the lack of fit (MSlof) and the Mean Square of the pure error (MSpe) was higher than the value of $F_{\text{tabulated}}$ (19.37) at the 95% confidence level. Although the model shows a lack of fit, this aspect does not compromise the results.

TABLE 1. Matrix of Central Composite Design with the Variables Evaluated for LIBS and Results Obtained from Overall Desirability (OD)

Experiment	Variables		OD
	Fluence, FL (J/cm ²)	Delay time, DT (μs)	
1	1811	0.7	0
2	3514	0.7	0.15
3	1811	1.7	0
4	3514	1.7	0.09
5 (CP)	2699	1.2	0.47
6 (CP)	2699	1.2	0.43
7 (CP)	2699	1.2	0.45
8	1448	1.2	0.36
9	3820	1.2	0.26
10	2699	0.5	0
11	2699	1.9	0

Equation (1) presents the obtained regression model with the significant coefficients and their confidence intervals at a confidence level of 95%, calculated as a function of OD, where b_0 is a constant and b_{22} (DT)² is the delay time:

$$\text{OD} = 0.445 \pm 0.272 - 0.246 \pm 0.198 (\text{DT})^2. \quad (1)$$

As b_0 was 0.445, this means that when both variables (FL and DT) are fixed at the central point, 0 and 0 (experiments 5, 6, and 7 at Table 1), an OD of around 0.4 can be obtained.

Negative signals in the quadratic coefficients for $(DT)^2$ show that there is a condition where a maximum exists. Fluency (b_1) was not a significant variable, which means any condition in the experimental domain studied is adequate. After the model calculation, it is possible to choose the conditions of commitment to the variables studied. According to the high OD values presented in Table 1, the appropriate conditions are in the central point, which corresponds to a delay time of 1.2 μ s and fluence of 2699 J/cm².

Calibration models. The calibration models were obtained using the reference values from ICP OES. As mentioned in the experimental section, a reference sample (NIST CRM 2709, San Joaquin Soil) was used in order to verify the accuracy of the proposed procedure for sample preparation and ICP OES determinations. After comparing the certified and determined values, a statistical evaluation was performed using unpaired Student *t*-test, and no significant difference between those values was observed at a 95% confidence level.

As the calibration strategy, matrix-matching calibration was used. For this strategy, a set of samples with concentrations determined by a reference technique, or certified reference materials, is used as solid calibration standards. One of the main advantages of the matrix-matching is that matrix effects can be minimized when the physical properties of the calibration standards are similar to the characteristics of the samples [28]. In this sense, the calibration models proposed for Ca, Fe, K, and Mg were obtained from 8 samples for the calibration set and 8 samples for the validation set.

In the case of quantitative analysis, LIBS has been criticized for producing less precise results than conventional atomic spectrometry techniques. To overcome these limitations, the use of normalizations strategies for the emission spectra has been reported in the literature [16–18]. In this sense, the raw spectra were submitted to twelve different normalization modes. These normalizations modes were assessed for several emission lines, and the best combination between the normalizations and the signals were selected according to the lowest SEC. The monitored emission lines (nm) were, for Ca: II 314.88, II 316.84, II 317.93, II 393.36, II 422.67, I 527.05, I 643.90, I 643.25, and I 649.37 nm; for Fe: II 259.94, II 273.95, II 274.74, II 274.94, 275.57, II 238.20; for K: I 766.49 and I 769.89; and for Mg: II 279.55, II 280.27, I 285.21, I 383.23, I 383.82, and I 518.36. These chosen using the Aurora software (Applied Spectra). It is necessary to evaluate several emission lines because the spectra generated via LIBS can have different spectral interferences for each analyte, and in addition, emission lines with lower signal intensity may give the best results [29].

After data normalizations, values of area and height were calculated for Ca, Fe, K, and Mg. The combination between the selected emission line (nm) for Ca II 393.36, Fe II 259.94, K I 766.49, and Mg II 279.55 using the area and height with the normalization mode that resulted in the lowest SEC are shown in Table 2. As can be observed, the SEC values for Ca, Fe, K, and Mg are statistically similar for all normalization modes. Thus, norm_5 (the sum of all the spectra) using the height for Ca, Fe, and Mg and the area for K was selected. Furthermore, the proposed models developed for LIBS gave about a 5-fold lower SEC compared to the samples with the lowest concentrations.

TABLE 2. Standard Error of Calibration (SEC) (mg/kg) using the Normalization Modes Proposed as Functions of Area and Height for Ca, Fe, K, and Mg

Normalization	Ca		Fe		K		Mg	
	Area	Height	Area	Height	Area	Height	Area	Height
Norm_1	204	184	4646	4363	273	314	95	96
Norm_2	218	212	5685	5378	301	344	126	116
Norm_3	211	205	5368	5101	293	337	117	108
Norm_4	219	210	6216	5798	324	368	123	114
Norm_5	205	185	4675	4388	273	314	95	96
Norm_6	218	212	5683	5373	300	343	125	116
Norm_7	211	205	5371	5100	291	336	116	108
Norm_8	219	209	6204	5784	322	367	122	113
Norm_9	259	239	4652	4084	248	299	118	127
Norm_10	260	240	4701	4134	246	298	118	127
Norm_11	253	235	3773	3501	264	295	121	128
Norm_12	254	235	3790	3512	263	294	120	129

Calibration models calculated for Ca, Fe, K, and Mg were prepared and evaluated using the validation data set. It was not possible to use a single set of calibration and validation because the concentrations range for elements vary greatly among the samples. Figure 2 present the reference and predicted concentrations for the calibration and validation data sets for the Ca. A good concordance was observed between both values obtained by ICP OES (reference values, squares) and the concentrations predicted by LIBS (circles)^{***}. In addition, it is possible to observe that the trueness for the calibration and validation data sets are in the range of 80–126%, confirming the good predictability of the proposed models (see bars). The trueness range (80–120%) is represented by the red line in the graph bars. The good trueness obtained demonstrate that the strategy of using the set of samples to propose the calibration models minimizes possible matrix effects. Several analytical parameters including the SEC, SEV, LOD, and LOQ were obtained. The SEC values were 185, 4839, 286, 95 (mg/kg); SEV were 190, 4188, 291, and 98 (mg/kg); LOD were 14, 16, 25, and 19 (mg/kg); and LOQ were 48, 55, 85, and 65 (mg/kg) for Ca, Fe, K, and Mg, respectively.

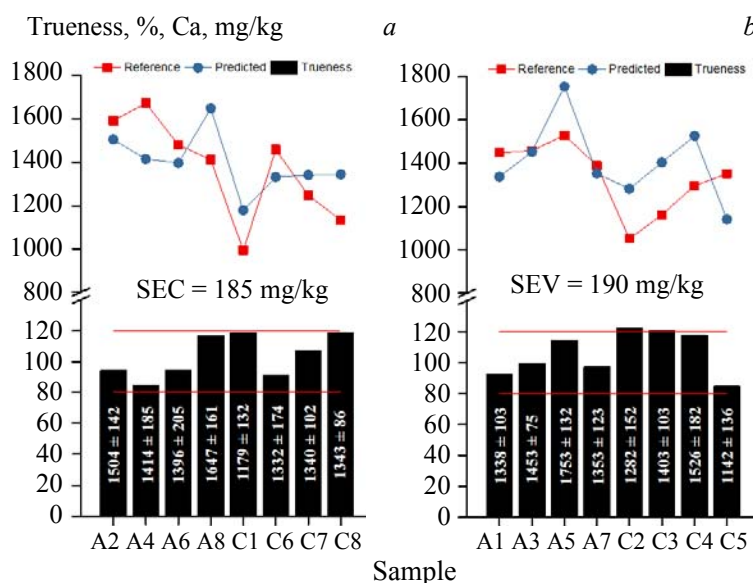


Fig. 2. Reference versus predicted concentrations for (a) calibration and (b) validation models for Ca, and trueness (%). The numbers presented inside the bars are the average and standard deviation of the predicted concentrations.

Multivariate data analysis using LIBS spectra. Multivariate data analysis from LIBS spectra in the region of 186–1042 nm for anthropized (A) and cabruca (C) soil samples from different depths (0–20 and 20–40 cm) was performed using PCA. In the PCA, data are projected into smaller matrices from the original data matrix by scores (samples) and loadings (variables). The scores show the distribution of the samples, and the loadings, the importance of the variables [30]. A data matrix of 16×12.288 (samples vs variables), after the data processing, generated four new principal components (PCs) PC1, PC2, PC3, and PC4, each one explaining 87.7, 6.5, 3.3, and 1.4%, respectively, of the total variability of the data.

Figure 3a shows the score plot of PC1×PC4, in which it is possible to observe four distinct clusters (A1 to A4; A5 to A8; C1 to C4 and C5 to C8) among the samples. Additionally, an ellipse with a 95% confidence interval was applied in PCA score plots, showing that the samples are within the 95% confidence limit. Figures 3b,c show the loadings for PC1 and PC4.

The clustering formed by samples A1 to A4 is dispersed in both PC1 and PC4. In PC1 two samples are on the positive side and two on the negative side, and the same behavior can be seen in PC4. The two samples that are on the positive side of PC1 and PC4 have high correlation with K, Mg, and Na, whereas the other two samples that are in the negative part of PC1 and PC4 have a correlation with Fe, Si and Ti. In PC1, the clustering formed by the samples A5 to A8 is influenced by K with positive loading values. In PC4, it is possible to verify positive clustering formed by the samples C1 to C4 and negative clustering formed

^{***} The results for the other analytes (K, Mg, and Na) can be obtained from authors.

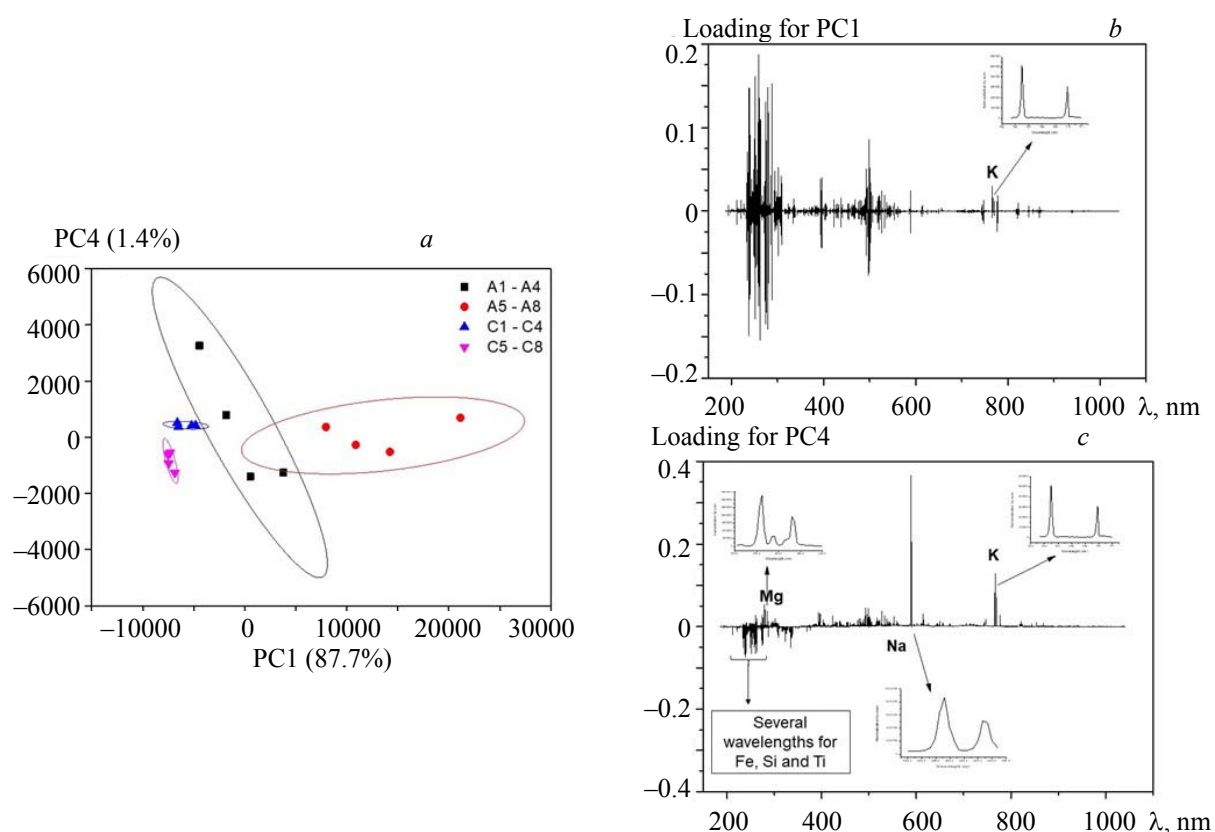


Fig. 3. Scores (a) and loadings for PC1 (b) and PC4 (c).

by the samples C5 to C8. Correlating Fig. 3a (scores) with Figs. 3b,c it is possible to observe that samples C1 to C4 present positive loading values for K, Mg, and Na, and samples C5 to C8 present negative loading values for Fe, Si, and Ti. From these results, it is concluded that the combination of LIBS analysis with PCA is an excellent option for the discrimination of soils.

Conclusions. The proposed method is fast and suitable for implementation in the direct determination of Ca, Fe, K, and Mg in soils. The normalization process of the raw data plays an important role in the quality of the results. The proposed models presented high prediction rates for the concentrations of Ca, Fe, K, and Mg with low SEC and LOD for calibration models. One of the advantages of the calibration models developed using samples as calibration standards is its matrix-matching capability. In addition, LIBS is adequate to discriminate the soil types studied. The use of PCA was fundamental for qualitative data interpretation. The analytical frequency of the proposed method is approximately 25 samples per hour, and the proposed method is environmentally friendly as fewer reagents, such as acids and solvents, are used, thus reducing waste.

Acknowledgments. This study was supported by the São Paulo Research Foundation (FAPESP, 2016/01513-0) and the Conselho Nacional de Desenvolvimento Científico e Tecnológico (CNPq, 401074/2014-5, 305637/2015-0, and 160152/2015-1). This study was financed in part by the Coordenação de Aperfeiçoamento de Pessoal de Nível Superior - Brasil (CAPES) - Finance Code 001.

REFERENCES

1. K. Mengel, K. A. Ernest, *Principles of Plant Nutrition*, 5th ed., Kluwer Academic Publ., Dordrecht (2001).
2. O. T. Butler, W. R. L. Cairns, J. M. Cook, C. M. Davidson, *J. Anal. At. Spectrom.*, **30**, 21 (2015).
3. F. J. Krug, F. R. P. Rocha, *Métodos de Preparo de Amostras. Fundamentos Sobre o Preparo de Amostras Orgânicas e Inorgânicas Para Análise Elementar*, Editora, EditSBQ, São Paulo (2016).

4. S. C. Jantzi, V. Motto-Ros, F. Trichard, Y. Markushin, N. Melikechi, A. Giacomo, *Spectrochim. Acta B*, **115**, 52 (2016).
5. J. El Haddad, L. Canioni, B. Bousquet, *Spectrochim. Acta B*, **101**, 171 (2014).
6. J. Yongcheng, S. Wen, Z. Baohua, L. Dongc, *J. Appl. Spectr.*, **84**, 731 (2017).
7. V. S. Burakov, S. N. Raikov, N. V. Tarasenko, M. V. Belkov, V. V. Kiris, *J. Appl. Spectr.*, **77**, 595 (2010).
8. M. J. C. Pontes, J. Cortez, R. K. H. Galvão, C. Pasquini, M. C. U. Araújo, R. M. Coelho, M. K. Chiba, M. F. Abreu, B. E. Madari, *Anal. Chim. Acta*, **642**, 12 (2009).
9. E. C. Ferreira, D. M. B. P. Milori, E. J. Ferreira, L. M. Santos, L. Martin-Neto, A. R. A. Nogueira, *Talanta*, **85**, 435 (2011).
10. E. C. Ferreira, E. J. Ferreira, P. R. Villas-Boas, G. S. Senesi, C. M. Carvalho, R. A. Romano, L. Martin-Neto, D. M. B. P. Milori, *Spectrochim. Acta B*, **99**, 76 (2014).
11. G. Nicolodelli, B. S. Marangoni, J. S. Cabral, P. R. Villas-Boas, G. S. Senesi, C. H. Santos, R. A. Romano, A. Segnini, Y. Lucas, C. R. Montes, D. M. B. P. Milori, *Appl. Opt.*, **53**, 2170 (2014).
12. P. R. Villas-Boas, R. A. Romano, M. A. M. Franco, E. C. Ferreira, E. J. Ferreira, S. Crestana, D. M. B. P. Milori, *Geoderma*, **263**, 195 (2016).
13. S. M. Zaytsev, I. N. Krylov, A. M. Popov, N. B. Zorov, T. A. Labutin, *Spectrochim. Acta B*, **140**, 65 (2018).
14. M. Rühlmann, D. Büchele, M. Ostermann, I. Bald, T. Schmid, *Spectrochim. Acta B*, **146**, 115 (2018).
15. P. Porízka, J. Klus, E. Képes, D. Prochazka, D. W. Hahn, J. Kaiser, *Spectrochim. Acta B*, **148**, 65 (2018).
16. J. P. Castro, E. R. Pereira-Filho, *J. Anal. At. Spectrom.*, **31**, 2005 (2016).
17. V. C. Costa, F. A. C. Amorim, D. V. Babos, E. R. Pereira-Filho, *Food Chem.*, **273**, 91 (2019).
18. V. C. Costa, F. W. B. Aquino, C. M. Paranhos, E. R. Pereira-Filho, *Polym. Test.*, **59**, 390 (2017).
19. M. Peña-Icart, E. R. Pereira-Filho, L. L. Fialho, J. A. Nóbrega, C. Alonso-Hernández, Y. Bolaños-Alvarez, *Chemosphere*, **168**, 1267 (2017).
20. A. M. Neiva, M. A. C. Jacinto, M. M. Alencar, S. N. Esteves, E. R. Pereira-Filho, *RSC Adv.*, **6**, 104827 (2016).
21. G. S. Senesi, R. A. Romano, B. S. Marangoni, G. Nicolodelli, P. R. Villas-Boas, V. M. Benites, D. M. B. P. Milori, *J. Appl. Spectr.*, **84**, 923 (2017).
22. CONAMA, 2009. Resolução nº 420, de 28 de dezembro de 2009. Brazil. Ministério do Meio Ambiente. DOU nº 249.
23. U. Epa, Microwave Assisted Acid Digestion of Siliceous and Organically Based Matrices, OHW, Method 3052 (1996).
24. M. A. Bezerra, R. E. Santelli, E. P. Oliveira, L. S. Villar, L. A. Escaleira, *Talanta*, **73**, 965 (2008).
25. L. V. Candiotti, M. M. Zan, M. S. Cámara, H. C. Goicoechea, *Talanta*, **124**, 123 (2014).
26. V. C. Costa, J. P. Castro, D. F. Andrade, D. V. Babos, J. A. Garcia, M. A. Sperança, T. A. Catelani, E. R. Pereira-Filho, *Trends Analyt. Chem.*, **108**, 65 (2018).
27. E. Tognoni, G. Cristoforetti, *Opt. Laser Technol.*, **79**, 164 (2016).
28. J. A. Carter, A. I. Barros, J. A. Nóbrega, G. L. Donati, *Front. Chem.*, **6**, 504 (2018).
29. A. S. Augusto, P. L. Barsanelli, F. M. V. Pereira, E. R. Pereira-Filho, *Food Res. Int.*, **94**, 72 (2017).
30. R. Bro, A. K. Smilde, *Anal. Methods*, **6**, 2812 (2014).